

Angular power spectrum of CMB anisotropy from WMAP

Tarun Souradeep¹, Rajib Saha^{1,2} and Pankaj Jain²

¹*Inter-University Centre for Astronomy and Astrophysics (IUCAA),*

Post Bag 4, Ganeshkhind, Pune 411 007, India.

E-mail: tarun@iucaa.ernet.in; rajib@iucaa.ernet.in

²*Physics Department, Indian Institute of Technology, Kanpur, U.P., 208016, India.*

E-mail: rajib@iitk.ac.in; pkjain@iitk.ac.in

Abstract

The remarkable improvement in the estimates of different cosmological parameters in recent years has been largely spearheaded by accurate measurements of the angular power spectrum of Cosmic Microwave Background (CMB) radiation. This has required removal of foreground contamination as well as detector noise bias with reliability and precision. Recently, a novel *model-independent* method for the estimation of CMB angular power spectrum from multi-frequency observations has been proposed and implemented on the first year WMAP (WMAP-1) data by Saha et al. 2006. We review the results from WMAP-1 and also present the new angular power spectrum based on three years of the WMAP data (WMAP-3). Previous estimates have depended on foreground templates built using extraneous observational input to remove foreground contamination. *This is the first demonstration that the CMB angular spectrum can be reliably estimated with precision from a self contained analysis of the WMAP data.* The primary product of WMAP are the observations of CMB in 10 independent difference assemblies (DA) distributed over 5 frequency bands that have uncorrelated noise. Our method utilizes maximum information available within WMAP data by linearly combining DA maps from different frequencies to remove foregrounds and estimating the power spectrum from the 24 cross power spectra of clean maps that have independent noise. An important merit of the method is that the expected residual power from unresolved point sources is significantly tempered to a constant offset at large multipoles (in contrast to the $\sim l^2$ contribution expected from a Poisson distribution) leading to a small correction at large multipoles. Hence, the power spectrum estimates are less susceptible to uncertainties in the model of point sources.

Key words: cosmology, theory, cosmic microwave background

1 Introduction

Remarkable progress in cosmology has been made due to the measurements of the anisotropy in the cosmic microwave background (CMB) over the past decade. The extraction of the angular power spectrum of the CMB anisotropy is complicated by foreground emission within our galaxy and extragalactic radio sources, as well, as the detector noise (1; 2). It is established that the CMB follows a blackbody distribution to high accuracy (3). Hence, foreground emissions may be removed by exploiting the fact that their contributions in different spectral bands are considerably different while the CMB power spectrum is same in all the bands (4; 5; 6; 7). Different approaches to foreground removal have been proposed in the literature (1; 2; 8; 9; 10).

The Wilkinson Microwave Anisotropy Probe (WMAP) observes in 5 frequency bands at 23 GHz (K), 33 GHz (Ka), 41 GHz (Q), 61 GHz (V) and 94 GHz (W). In the first data release, the WMAP team removed the galactic foreground signal using a template fitting method based on a model of synchrotron, free free and dust emission in our galaxy (6). The sky map around the galactic plane and around known extragalactic point sources were masked out and the CMB power spectrum was then obtained from cross power spectra of independent difference assemblies in the 41 GHz, 61 GHz and 94 GHz foreground cleaned maps (12).

A model independent removal of foregrounds has been proposed in the literature (2). The method has also been implemented on the WMAP data in order to create a foreground cleaned map (13). The main advantage of this method is that it does not make any additional assumptions regarding the nature of the foregrounds. Furthermore, the procedure is computationally fast. The foreground emissions are removed by combining the five different WMAP bands by weights which depend both on the angular scale and on the location in the sky (divided into regions based on ‘cleanliness’). However, the power spectrum recovered from the single foreground cleaned map has severe excess power at large multipole moments due to amplification of detector noise bias in the autocorrelation power spectrum beyond the beam resolution.

The prime objective of our method (11) is to adapt and extend the foreground cleaning approach to power spectrum estimation by retaining the ability to remove detector noise bias exploiting the fact that it is uncorrelated among the different Difference Assemblies (DA) (12; 14). The WMAP data uses 10 DA’s (15; 16; 17; 18), one each for K and Ka bands, two for Q band, two for V band and four for W band. We label these as K, Ka, Q1, Q2, V1, V2, W1, W2, W3, and W4 respectively. We eliminate the detector noise bias using cross power spectra and provide a model independent extraction of CMB power spectrum from WMAP first year data. So far, only the three highest frequency channels

observed by WMAP have been used to extract CMB power spectrum and the foreground removal has used foreground templates based on extrapolated flux from measurements at frequencies far removed from observational frequencies of WMAP (12; 19; 20). We present a more general procedure where we use observations from all the five frequency channels of WMAP and do not use any observational input extraneous to the WMAP data set.

2 Methodology

The entire method can be neatly split into three distinct sections –

- foreground cleaning,
- power spectrum estimation, and,
- correcting for known systematics.

We discuss in some detail the systematic correction for residual power due to unresolved sources ¹. A merit of our approach is that the expected residual power in the cross spectra from combined maps has a flat dependence with increasing multipoles – a strongly tempered dependence given that the contribution in individual DA maps scales as l^2 . (This feature holds promise for experiments at higher angular resolution.)

The three parts of the current methodology are logically modular and it is possible to modify and improve each one relatively independent of the other. Specifically, we have employed the Pseudo- C_l (MASTER (23)) power spectrum estimation from the foreground cleaned maps which is fast but sub-optimal for the low l (in practice). More appropriate approaches have been proposed (24; 25; 26). We are exploring improvements on this front.

2.1 Foreground Cleaning

The foreground cleaning stage of our method is adapted from Tegmark & Efstathiou (1996) and Tegmark *et al.* (2003). In Tegmark *et al.* (2003), a foreground cleaned map is obtained by linearly combining 5 maps corresponding to one each for the different WMAP frequency channels. For the Q, V and W frequency channels, where more than one maps were available, an averaged map was used. However, averaging over the DA maps in a given frequency channel precludes any possibility of removing detector noise bias using cross correlation. In our method we linearly combine maps corresponding to a set of 4 DA maps at different frequencies. We treat K and Ka maps effectively

¹ Study of other effects, such as beam non-circularity is in progress (21; 22).

(K,KA)+Q1+V1+W12=(C1,CA1)	(K,KA)+Q1+V2+W12=(C13,CA13)
(K,KA)+Q1+V1+W13=(C2,CA2)	(K,KA)+Q1+V2+W13=(C14,CA14)
(K,KA)+Q1+V1+W14=(C3,CA3)	(K,KA)+Q1+V2+W14=(C15,CA15)
(K,KA)+Q1+V1+W23=(C4,CA4)	(K,KA)+Q1+V2+W23=(C16,CA16)
(K,KA)+Q1+V1+W24=(C5,CA5)	(K,KA)+Q1+V2+W24=(C17,CA17)
(K,KA)+Q1+V1+W34=(C6,CA6)	(K,KA)+Q1+V2+W34=(C18,CA18)
(K,KA)+Q2+V2+W12=(C7,CA7)	(K,KA)+Q2+V1+W12=(C19,CA19)
(K,KA)+Q2+V2+W13=(C8,CA8)	(K,KA)+Q2+V1+W13=(C20,CA20)
(K,KA)+Q2+V2+W14=(C9,CA9)	(K,KA)+Q2+V1+W14=(C21,CA21)
(K,KA)+Q2+V2+W23=(C10,CA10)	(K,KA)+Q2+V1+W23=(C22,CA22)
(K,KA)+Q2+V2+W24=(C11,CA11)	(K,KA)+Q2+V1+W24=(C23,CA23)
(K,KA)+Q2+V2+W34=(C12,CA12)	(K,KA)+Q2+V1+W34=(C24,CA24)

Table 1

List of the 48 possible combinations of the DA maps that lead to 48 cleaned maps (Ci, CAi), i=1,2,...,24..

as the observation of CMB in two different DA (at the lowest frequencies). Therefore we use K and Ka maps in separate combinations. In case of W band 4 DA maps are available. We simply form an averaged map taking two of them at a time and form effectively 6 DA maps corresponding to W band. W_{ij} represents simply an averaged map obtained from the i^{th} and j^{th} DA of W band ². In table 1 we list all the 48 possible linear combinations of the DA maps that lead to ‘cleaned’ maps, Ci and CAi’s, where $i = 1, 2, \dots, 24$.

The goal is to determine a set of optimal weights for each multipole,

$$[\mathbf{W}_1] = (w_l^1, w_l^2, w_l^3, w_l^4) \quad (1)$$

that specifies the linear combination of 4 DA in the combination, which lead to a ‘cleaned’ map with minimal power

$$a_{lm}^{\text{Clean}} = \sum_{i=1}^{i=4} w_l^i \frac{a_{lm}^i}{B_l^i}, \quad (2)$$

where a_{lm}^i is spherical harmonic transform of map and B_l^i is the appropriate beam function for the channel i . The condition that the achromatic CMB signal remains untouched during cleaning is encoded as the constraint

$$[\mathbf{W}_1][\mathbf{e}] = [\mathbf{e}]^T[\mathbf{W}]^T = \mathbf{1}, \quad (3)$$

² Other variations are possible and some explored. We defer a discussion to a more detailed publication (27).

where $[\mathbf{e}] = (1, 1, 1, 1)^T$ is a 4×1 column vector with unit elements. The constraint implies that the total power in the cleaned map

$$C_l^{Clean} = [\mathbf{W}_l][\mathbf{C}_l][\mathbf{W}_l]^T = C_l^S + [\mathbf{W}_l][\mathbf{C}_l^{(\mathbf{R})}][\mathbf{W}_l]^T \quad (4)$$

where C_l^S is the CMB power spectrum and the last term is the unwanted (non-cosmic, frequency dependent) contribution from the foreground and other contaminants.

The optimum weights to combine 4 different frequency channels such as to minimize the second term on the *rhs* of eq. 4 subject to the constraint that CMB is untouched (eq. 3) is readily obtained as (2; 13)

$$[\mathbf{W}_l] = [\mathbf{e}]^T[\mathbf{C}_l]^{-1} / ([\mathbf{e}]^T[\mathbf{C}_l]^{-1}[\mathbf{e}]) . \quad (5)$$

Here the matrix

$$[\mathbf{C}_l] \equiv C_l^{ij} = \frac{1}{2l+1} \sum_{m=-l}^{m=l} \frac{a_{lm}^i a_{lm}^{j*}}{B_l^i B_l^j} . \quad (6)$$

In practice, we smooth all the elements of the \mathbf{C}_l using a moving average window over $\Delta l = 11$ before deconvolving by the beam function. This avoids the possibility of an occasional singular \mathbf{C}_l that cannot be inverted. The entire cleaning procedure is automated and takes approximately 3 hours on a 16 alpha processor machine to get the 48 cleaned maps. In all the 48 maps some residual foreground contamination is visibly present along a small narrow strip on the galactic plane. For the angular power estimation that follows, the Kp2 mask employed suffices to mask the contaminated region in all the 48 maps. In ongoing work, we assess the quality of foreground cleaning in these maps using the Bipolar power spectrum method (28; 29; 30; 31).

2.2 Power Spectrum Estimation

Independent estimates of the power spectrum can be obtained by cross correlation power spectra

$$C_l^{ij} = (2l+1)^{-1} \sum_m a_{lm}^i (a_{lm}^j)^* \quad (7)$$

of pairs of cleaned maps \mathbf{C}_i & \mathbf{C}_j chosen such that they share no common DA. This ensures a zero noise bias of the estimates. A Kp2 mask is applied to the maps to mask out foreground contaminated regions and accounted

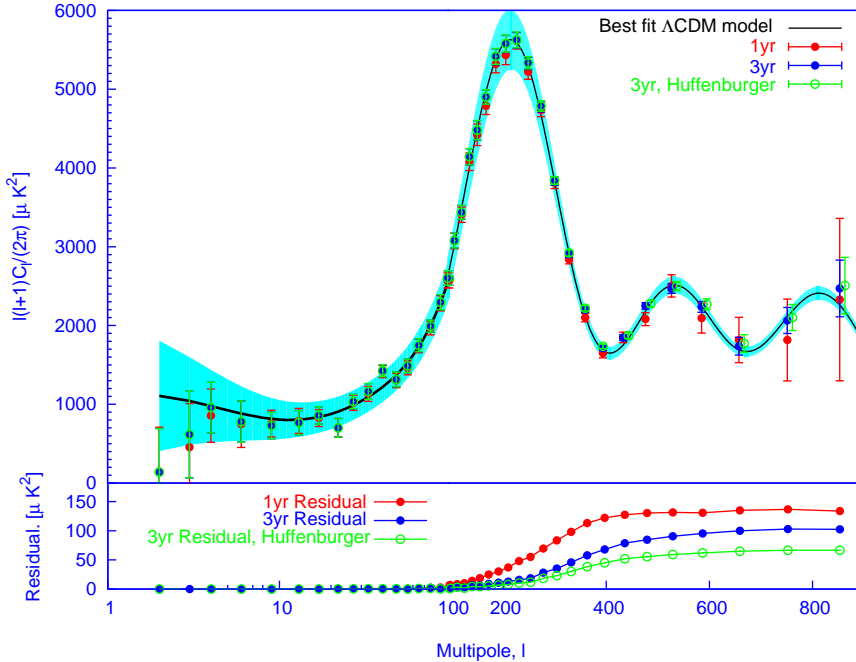


Fig. 1. The final angular power spectrum from WMAP-1 (red) and WMAP-3 (blue & green) data are shown in the upper panel. The lower panel shows the correction made for the residual power from unresolved point sources based on the point source models published by WMAP team for the corresponding year. The green curve in the panels correspond to the WMAP-3 spectrum (upper), and the corresponding correction (lower) obtained using a revised point source model suggested by Huffenberger et al. 2006. Note the tempered behavior of the point source correction in our method (also see fig. 4). The multipole range is log scale for $l < 100$, and linear, thereafter.

for by de-biasing the pseudo- C_l estimate using the coupling (bias) matrix corresponding to the Kp2 mask, appropriate circularized beam transform and pixel window (23). The left panel of figure 2 plots and lists the 24 cross power spectra for which the noise bias is zero and closely match each other for $l < 540$. (This is in contrast to pre-point source corrected cross power spectra in WMAP-1 power spectrum estimation shown in the right panel – a merit of our method that we discuss in the next section.)

An ‘Uniform average’ power spectrum is then obtained by combining the 24 cross power spectra with equal weights³. The power spectrum is then corrected for residual power from unresolved point sources as described in the next subsection. The error bars have been estimated with comprehensive simulations described in §2.4. The final power spectrum is binned in the same manner as the WMAP’s published result for ease of comparison.

³ There exists the additional freedom to choose optimal weights for combining the 24 cross-power spectra.

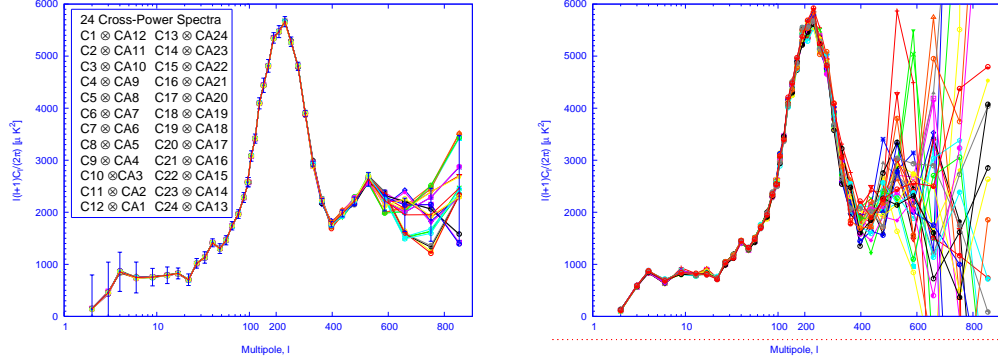


Fig. 2. *Left*: Plot of the 24 individual cross power spectra corresponding to the cross correlations listed in this figure are show very small dispersion for $l \lesssim 540$. The average power spectrum is plotted in red line and blue error bars. *Right*: Plot of the 28 cross-power spectra in the WMAP-1 team analysis prior to point source corrections show a large scatter at large l . The multipole range is log scale for $l < 100$, and linear, thereafter.

The power spectra from our independent analyzes is entirely consistent with the WMAP-1 (12; 11) and WMAP-3 (32; 33) team results. We find a suppression of power in the quadrupole and octopole moments consistent with WMAP-1 published result. However, in WMAP-1 our quadrupole moment ($146\mu K^2$) is a little larger than WMAP-1 result ($123\mu K^2$) and Octopole ($455\mu K^2$) is less than WMAP-1 result ($611\mu K^2$). Our WMAP-1 spectrum does not show the ‘bite’ like feature present in WMAP’s power spectrum at the first acoustic peak reported by WMAP-1 (12). In the three year results, the differences at low $l \leq 10$ between WMAP result and our is primarily due to the fact that WMAP report the maximum likelihood values for $l \leq 10$ (and we employ pseudo- C_l estimation). At large l , our results are consistent with other estimates as shown in a comprehensive reanalysis of WMAP-3 carried out jointly with five independent, international CMB analysis groups (see MASTERint in Ref. (33)).

A quadratic fit to the peaks and troughs of the binned WMAP-1 [WMAP-3] power spectrum shown in the figure 3, locates the first acoustic peak at $l = 219.8 \pm 0.8$ [219.9 ± 0.8] with amplitude $\Delta T_l = 74.1 \pm 0.3$ [74.4 ± 0.3] μK , the second acoustic peak at $l = 544 \pm 17$ [539.5 ± 3.8] with amplitude $\Delta T_l = 48.3 \pm 1.2$ [49.4 ± 0.4] μK and the first trough at $l = 419.2 \pm 5.6$ [417.7 ± 3.2] with amplitude $\Delta T_l = 41.7 \pm 1$ [41.3 ± 0.6] μK .

2.3 Residual unresolved point source correction

The residual power contamination in the ‘Uniform average’ power spectrum from unresolved point sources can be estimated by running through our analysis the frequency dependent power obtained from the same source model

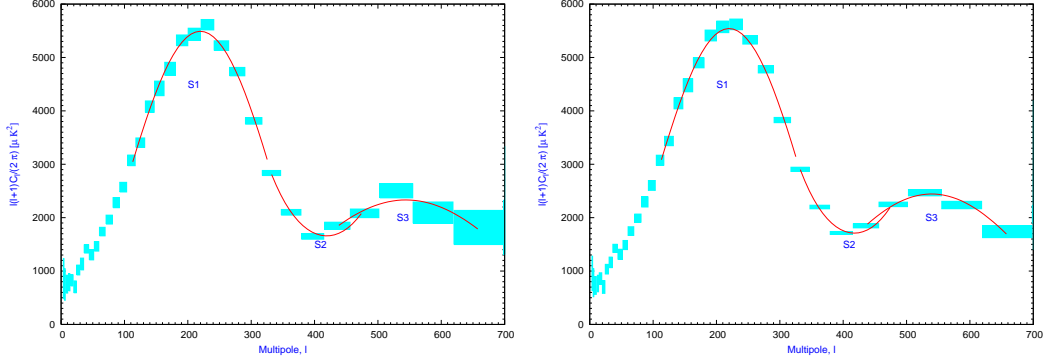


Fig. 3. The red line shows the quadratic function fitted to the peaks and troughs of the final binned angular power spectrum for WMAP-1 data (left) and WMAP-3 (right). S1, S2 and S3 are the 3 different sections of the spectrum on which fits are performed individually. The power spectrum estimates with error bars and multipole band are represented as the shaded boxes.

used by WMAP team to correct for this contaminant (12; 32). WMAP has a fitted a simple model with a constant spectral index over the entire sky for the residual power in cross-spectra $C_l^{(PS)ij}$ of frequency channel i and j from unresolved point sources as (6)

$$C_l^{(PS)ij} = A \left(\frac{\nu_i}{\nu_0} \right)^\beta \left(\frac{\nu_j}{\nu_0} \right)^\beta \quad (8)$$

The amplitude A and slope $\beta \approx -2$ has been obtained by extrapolation from the fluxes and spectra of 208 resolved point sources in the WMAP-1 (6) and 300 point sources in WMAP-3 (32).

The contribution from each region $\alpha = 1, 2, \dots, 9$ to the expected residual from unresolved point sources in our cross-power spectrum of cleaned maps \mathbf{i} and \mathbf{j} which are each linear combinations of 4 DA's at different frequencies (eq. 2) is given by

$$C_l^{(PS)\alpha\mathbf{ij}} = \sum_{i=1}^4 \sum_{j=1}^4 w_l^i(\mathbf{i}) w_l^j(\mathbf{j}) A \left(\frac{\nu_i}{\nu_0} \right)^{-2} \left(\frac{\nu_j}{\nu_0} \right)^{-2}, \quad (9)$$

where $w_l^i(\mathbf{i})$ denotes the weight vector for the cleaned map \mathbf{i} and ν_0 is a fiducial frequency. The index pair (\mathbf{ij}) are effectively a single index limited to the 24 'allowed' cross-spectra. The total contribution is added up as

$$C_l^{(PS)} = (1/24) \sum_{(\mathbf{ij})=1}^{24} \sum_{\alpha} \sum_{l'} M_{ll'}^{(\alpha)} C_{l'}^{(PS)\alpha\mathbf{ij}} \quad (10)$$

where $M_{ll'}^\alpha$ the coupling matrix for the individual regions where $\alpha = 1, 2, \dots, 9$.

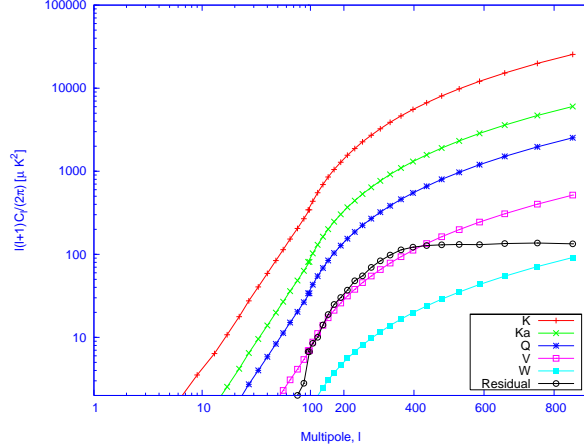


Fig. 4. Comparison of the residual power in WMAP due to unresolved point source contamination (black) in the final averaged cross power spectra in our method with the actual level point source contamination in each the 5 frequency channels. Note that the level of residual contamination is in between the cleanest (highest) two frequency channels (V & W). More importantly, the residual point source correction is constant with multipoles whereas the actual level of contamination increases $\propto l^2$ with multipoles. This implies that our method is efficient in canceling out the point source contamination at high resolution.

We use the above expression to estimate the unresolved residual point source contamination in the final cross power spectrum. We note in passing that this estimation is entirely based upon the assumption that the residual unresolved point source contamination is statistically isotropic over the sky. The residual power from unresolved point sources in WMAP-1 [WMAP-3] is a constant offset of ~ 140 [100] μK^2 for $l \gtrsim 400$ (and negligible at lower l). As seen in figure 4, this residual is much less than actual point source contamination in Q, KA or K band and intermediate between V and W band point source contamination. It is noteworthy that the method significantly tempers the point source residual at large l that otherwise is $\propto l^2$ in each map.

2.4 Error Estimate on the Power Spectrum

The errors on the final power spectrum are computed from Monte Carlo simulations of CMB maps for every DA each with a realization of the WMAP noise and common signal and diffuse foreground contamination. For WMAP-1, we use the 110 random noise maps made available at the LAMBDA data archive. For WMAP-3 year analysis random noise map corresponding to each DA are generated by first sampling a Gaussian distribution with unit variance. In the final step we multiply each Gaussian variable by the number $\sigma_0/\sqrt{N_p}$ to form realistic noise maps. Here σ_0 is the noise per observation for the DA under consideration and $\sqrt{N_p}$ is the effective number of observations at each pixel. We use the publicly available Planck Sky Model to simulate the con-

tamination from the diffuse galactic (synchrotron, thermal dust and free-free) emission at the WMAP frequencies. The CMB maps were smoothed by the beam function appropriate for each WMAP’s detector. The set of realistic DA maps with noise, foreground and CMB are then passed through the cleaning pipeline. The common CMB signal in all the maps was based on a realization of the WMAP ‘power law’ best fit Λ -CDM model (34). Averaging over the power spectra from the simulations we recover the model power spectrum, but for a hint of bias towards lower values in the low l moments. For $l = 2$ and $l = 3$ the bias is -27.4% and -13.8% respectively. However this bias become negligible at higher l , e.g. at $l = 22$, it is only -0.8% .

The standard deviation obtained from the diagonal elements of the covariance matrix is used as the error bars on the C_l ’s obtained from the data ⁴. The covariance matrix of the binned power spectrum is largely diagonal.

3 Conclusion

The rapid improvement in the sensitivity and resolution of the CMB experiments has posed increasingly stringent requirements on the level of separation and removal of the foreground contaminants. Standard approaches to foreground removal, usually attempt to incorporate the extra information about the amplitude, spatial structure and distribution of foregrounds available at other frequencies, in constructing a foreground template at the frequencies of the CMB measurements. These approaches could be susceptible to uncertainties and inadequacies of modeling involved in extrapolating from the frequency of observation to CMB observations.

We carry out an estimation of the CMB power spectrum from the WMAP data that is independent of foreground model and evades these uncertainties. The novelty is to make clean maps from the difference assemblies and exploit the lack of noise correlation between the independent channels to eliminate noise bias. *This is the first demonstration that the angular power spectrum of CMB anisotropy can be reliably estimated with precision solely from the WMAP data (difference assembly maps) without recourse to any external data.* Our work is a clear demonstration that the blind approach to foreground cleaning is comparable in efficiency to that from template fitting methods and certainly adequate for a reliable estimation of the angular power spectrum. Moreover, this method enjoys the advantage of eliminating the uncertainties of modeling required to create the foreground templates that estimate the contamination at the CMB dominated frequencies by extrapolating from the observed emission

⁴ The beam uncertainty is not included here, but is deferred to future work where we also incorporate non-circular beam corrections (21).

flux at very different frequencies where the foregrounds dominate.

Further, the tempered, flat, large l behavior of residual from unresolved point sources in this method holds promise for experiment with finer angular resolution. The understanding of polarized foreground contamination in CMB polarization maps is rather scarce. Hence modeling uncertainties could dominate the systematics error budget of conventional foreground cleaning. The blind approach extended to estimating polarization spectra after cleaning CMB polarization maps could prove to be particularly advantageous.

Acknowledgment

The analysis pipeline as well as the entire simulation pipeline is based on primitives from the Healpix package ⁵. We acknowledge the use of version 1.1 of the Planck reference sky model, prepared by the members of Working Group 2 and available at www.planck.fr/healing79.html. The entire analysis procedure was carried out on the IUCAA HPC facility. RS thanks IUCAA for hosting his visits. We thank the WMAP team for producing excellent quality CMB maps and making them publicly available. We thank Amir Hajian, Subharthi Ray and Sanjit Mitra in IUCAA for helpful discussions. We are grateful to Lyman Page, Olivier Dore, Francois Bouchet, Simon Prunet, Charles Lawrence, Kris Gorski and Max Tegmark for thoughtful comments and suggestions on this work.

References

- [1] F. R. Bouchet and R. Gispert, *New Astronomy* **4**,443, (1999).
- [2] M. Tegmark, G. Efstathiou *Mon. Not. R. Astron. Soc.*, **281**, 1297, (1996).
- [3] J. Mather *et al.*, *Astrophys. J.*, **420**, 439, (1994); *ibid.* **512**, 511 (1999).
- [4] S. Dodelson, *Astrophys. J.*, **482**, 577 (1997).
- [5] M. Tegmark, D. J. Eisenstein, W. Hu, & A. de-Oliveira-Costa, *Astrophys. J.*, **530**, 133, (2000).
- [6] C. L. Bennett *et al.*, *Astrophys. J. Supp.*, **148**, 97 (2003).
- [7] M. Tegmark, *Astrophys. J.* **502** 1, (1998).
- [8] M. P. Hobson *et al.*, *Mon. Not. R. Astron. Soc.*, **300** 1 (1998).
- [9] D. Maino *et al.*, *Mon. Not. R. Astron. Soc.*, **334**, 53 (2002); *ibid.* **344**, 544 (2003).
- [10] H. K. Eriksen *et al.*, *Astrophys. J.* **641**, 665, (2006).
- [11] R. Saha, P. Jain & T. Souradeep, *Astrophys. J. Lett.*, **645**, L89, (2006).

⁵ The Healpix distribution (35) is publicly available from the website <http://www.eso.org/science/healpix>.

- [12] G. Hinshaw *et al.*, *Astrophys. J. Supp.*, **148**, 135 (2003).
- [13] M. Tegmark, A. de Oliveira-Costa & A. Hamilton, *Phys. Rev. D* **68**, 123523 (2003).
- [14] N. Jarosik *et al.*, *Astrophys. J. Supp.* **145**, 413 (2003).
- [15] C. L. Bennett *et al.*, *Astrophys. J. Supp.* **148**, 1 (2003).
- [16] C. L. Bennett *et al.*, *Astrophys. J.*, **583**, 1 (2003).
- [17] M. Limon, *et al.*, Wilkinson Microwave Anisotropy Probe (WMAP): Explanatory Supplement, version 1.0, at the LAMBDA website.
- [18] G. Hinshaw *et al.* *Astrophys. J. Supp.*, **148**, 63 (2003).
- [19] P. Fosalba & I. Szapudi, *Astrophys. J.*, **617**, 95 (2004).
- [20] G. Patanchon, J. F. Cardoso, J. Delabrouille & P. Vielva, *preprint* [arXiv: astro-ph/0410280].
- [21] S. Mitra, A. S. Sengupta and T. Souradeep, *Phys. Rev. D.* **70** 103002 (2004).
- [22] T. Souradeep, S. Mitra, A. S. Sengupta, S. Ray and R. Saha, (*in these proceedings*).
- [23] E. Hivon *et al.*, *Astrophys. J.* **567**, 2 (2002).
- [24] L. Knox, N. Christensen & C. Skordis, *Astrophys. J.* **563**, L95, (2001).
- [25] J. Jewell, S. Levin & C. H. Anderson, *Astrophys. J.* **609**, 1, (2004).
- [26] B. D. Wandelt, D. L. Larson & A. Lakshminarayanan, *Phys. Rev. D.* **70**, 083511 (2004).
- [27] R. Saha, P. Jain, & T. Souradeep, *in preparation*.
- [28] A. Hajian & T. Souradeep, *Astrophys. J.*, **597**, 5 (2003).
- [29] A. Hajian *et al.* *Astrophys. J.*, **618**, 63 (2004).
- [30] A. Hajian, T. Souradeep, *preprint* [arXiv: astro-ph/0501001].
- [31] S. Basak, A. Hajian & T. Souradeep, (*in these proceedings*), [arXiv: astro-ph/0607577]
- [32] G. Hinshaw *et al.*, *preprint* [arXiv: astro-ph/0603451].
- [33] H. K. K. Eriksen *et al.*, *preprint* [arXiv: astro-ph/0606088].
- [34] D. Spergel *et al.*, *Astrophys. J. Suppl.*, **148**, 175, (2003); *ibid preprint* [arXiv: astro-ph/0603449].
- [35] K. M. Gorski *et al.*, [arXiv: astro-ph/9905275]; Gorski, K. M. *et al.* [arXiv: astro-ph/9812350].